Sensors and Materials, Vol. 34, No. 5 (2022) 1733–1746
MYU Tokyo

S & M 2924

Design and Analysis of New Electric Motorcycle: Analysis of Bending Moment Stiffness

Hong-Mei Dai,[1] Bo-Hao Chen,[2] Chao-Ming Hsu,[2*] and Cheng-Fu Yang[3,4**]

[1]College of Art, Zhongqiao Vocational and Technical University, Shanghai 201514, China
[2]Department of Mechanical Engineering, National Kaohsiung University of Applied Science, Kaohsiung 807, Taiwan
[3]Department of Chemical and Materials Engineering, National University of Kaohsiung, Kaohsiung 811, Taiwan
[4]Department of Aeronautical Engineering, Chaoyang University of Technology, Taichung 413, Taiwan

(Received December 30, 2021; accepted March 22, 2022)

Keywords: frame structure, simulation analysis, electric motorcycle, finite element method

When an electric motorcycle is being driven, its frame structure needs to bear not only the loads of the motorcycle components and the driver, but also the load from the road surface. If the road condition is poor, the frame will transmit the rebound force from the road through the front and rear wheels and suspension system, which is the main cause of the deformation of the frame structure. Therefore, the frame structure must have sufficient rigidity to withstand these external loads, so that the permanent deformation of the frame structure can be avoided, which would affect the fixation of the other components in the motorcycle. These are serious problems because they reduce the vehicle handling performance and threaten the safety of drivers. In this study, we analyzed the upper and lower bending moment stiffnesses, left and right bending moment stiffnesses, and front and rear bending moment stiffnesses of a newly designed electric motorcycle. We mainly used ANSYS as the finite element method (FEM) software to simulate and analyze the motorcycle. After a model for the motorcycle was constructed, FEM was used to predict and analyze the force mode of the proposed prototype structure; the simulations and analyses of force modes included the frame rigidity and the frame structure strength. FEM technology was also used to explore the force applied to the frame under different load conditions. In the case of deformation, the simulation technology found a part of the newly designed electric motorcycle's structure that needed to be strengthened and the optimal size of the prototype frame structure.

1. Introduction

According to statistics from the Ministry of Transport of Taiwan, more than 14 million motorcycles are owned by the 23 million people of Taiwan, and there are more than 419 motorcycles per square kilometer.[(1)] In recent years, with the increased focus on environmental issues, more styles and types of electric motorcycles have become available, which can be used

*Corresponding author: e-mail: jammy@kuas.edu.tw
**Corresponding author: e-mail: cfyang@nuk.edu.tw
https://doi.org/10.18494/SAM3819

ISSN 0914-4935
https://myukk.org/

as alternatives to gasoline-fueled motorcycles. Many new electric motorcycle brands with various designs and appearances to meet the needs of different consumers are currently being developed in Taiwan. Electric motorcycles have evolved from being bulky and lacking in range to attractive lightweight models with a longer range. Also, the structures of newly designed electric motorcycles are now comparable to those of gasoline-fueled motorcycles. Because of the Taiwanese government's vigorous promotion of subsidies for electric motorcycles, consumers have been encouraged to purchase new electric motorcycles to replace gasoline-fueled motorcycles. The rapid increase in the demand for electric motorcycles has encouraged businesses to import a large number of electric motorcycles.

The electric motorcycles sold in Taiwan are mainly made in Taiwan and China, but their quality is markedly different. For many of the designs, the structural strength and durability have not been carefully evaluated. Therefore, some electric motorcycles have short service lives or their frame must be replaced immediately after light collisions. Although the use of electric motorcycles contributes to the reduction of carbon emissions, some of them have structural issues, resulting in a high damage rate and replacement rate of the parts. Therefore, the aim of our research is to contribute to the establishment of a set of evidence-based frame-testing procedures so that new electric motorcycles with improved service life can be designed using the finite element method (FEM). Electric motorcycles with a well-designed body can also achieve a similar energy-saving and carbon-emission-reducing effect. Moreover, commercial software for designing and simulating new transportation vehicles has become an important technology because it can reduce the workload of engineers and increase transportation safety.(2,3)

Tuluie and Ericksen created a CAD solid model of a motorcycle, and a virtual dynamic model with various parameters was used in their proposed model to perform simulations of sine sweep, noise, and road driving.(4) Their proposed solid mode was used to measure loads and other dynamic responses on the virtual model to optimize the design of a motorcycle and obtain acceptable performance and durability. Recently, FEM was used to simulate the model of a motorcycle body structure, and the technology of simulation analysis provided the research direction for the designers to modify and obtain a better structural design.(5,6) The simulation parameters included the dynamic and static analysis data and the optimization design of the motorcycle body structure. In dynamic analysis, when FEM software is used to find the natural vibration frequency of the structure of a motorcycle body, the simulation results are used to verify the model-based experiment to ensure the reliability of the FEM analysis model. In static analysis, when the software is used to simulate the force and deformation of a motorcycle body structure, the simulation results are used to find the positions where the frame structure needs to be strengthened. Finally, a parameterized design is given to the structure and the optimal design of the structure is obtained.

Sheu developed a new hybrid motorcycle, established an analysis model, and used software to simulate it with the aim of studying the performance and optimizing the fuel economy of a proposed hybrid power system.(7) The simulation results verified the operating capability of the hybrid power system, and the engine and electric motor were adjusted to the optimal settings under various operating conditions. In 2015, Marzuki *et al.* used ANSYS Design Modeler to establish a geometric model of the frame of a racing car and analyze the natural vibration mode of the frame. They confirmed that this model was consistent with the appearance of the geometric model.[8] The parameters obtained from the simulation results confirmed that the natural vibration level of the car frame did not affect the driver or the frame. These results suggest that simulation technology is an important method for designing an electric motorcycle or car with high bending moment stiffness.

The FEM analysis used at present originated from research on elasticity and structural analyses in civil engineering and aviation engineering. In this study, we mainly used ANSYS as the FEM software to simulate and analyze a new electric motorcycle design. After the model of the electric motorcycle was designed, we used FEM to predict and analyze the force modes of the proposed prototype structure. The novelty of this study is that we designed a new electric motorcycle and analyzed its force modes using a simulation method. This process can save money and time by eliminating the need to actually build an electric motorcycle.

The initial stage of the motorcycle design in the simulation process was to construct the main frame, and the most important consideration in the design was the rigidity of the main frame. The overall frame structure mainly comprised the main frame, seat tube, rear rocker arm, front shock absorber, and rear shock absorber, which were supported by front and rear wheels. At present, the common frame materials on the market include cast iron, cast steel, alloy steel, magnesium alloy, aluminum alloy, and titanium alloy. Differences in the purchase cost of motorcycles with materials of different strengths are unavoidable. Rigidity tests with consideration of different types of drivers are very important, because they will affect the durability of the overall structure of the electric motorcycle and whether it can ensure the safety of the driver. In this study, we analyzed the upper and lower bending moment stiffnesses, left and right bending moment stiffnesses, and front and rear bending moment stiffnesses of a newly designed electric motorcycle. The traditional method of analysis uses sensors to detect the force patterns of a fabricated electric motorcycle body. However, the simulation method can replace the traditional method, i.e., reduce the use of sensors. We used A36 structural steel, which is commonly used on the market, to design and optimize the structure of a newly designed electric motorcycle with the aim of reducing the cost of an electric motorcycle while maintaining the frame strength.

2. Simulation Process and Parameters

The modules and theories used for the newly designed electric motorcycle were mainly for the static structural analyses of the frame. The frame is the structural component that mainly bears the load, and it is composed of two or more rigidly connected beams because its longitudinal dimension is greater than the two transverse dimensions. Deformation of the frame beam is mainly caused by bending in the lateral direction, and bending-dominated deformation is the main mechanism by which the frame beam resists the load. Under the assumption that the length of the neutral axis is constant, the material layer located along the axis remains stress-free, but the beam bends upwards to resist downward lateral loads. The bending frame causes the layer above the intermediate shaft to compress axially and stretch downward in the axial direction. The material layer further from the neutral axis is tighter and the strain is greater. The axial strain caused by bending is called the bending strain, and the geometric difference related to the deflection curvature $\kappa(x)$ is as follows:

$$\varepsilon(x) = -y\kappa(x) = -y\frac{d^2v}{dx^2}, \tag{1}$$

where y is the vertical distance between the beam and the neutral axis and v is the deflection. From the theory of elasticity, the internal bending moment $M(x)$ is a function of the axial bending stress $\sigma(x)$. Applying this principle to Eq. (1), we obtain

$$M(x) = \int -y\sigma(x)dA = \int Ey^2\kappa(x)dA = EI\kappa(x) = EI\frac{d^2v}{dx^2}, \tag{2}$$

where E is the elastic modulus of the material, I is the area moment of inertia of the beam cross section relative to the z-axis, and the product of E and I is called the bending stiffness. By combining the equations, the bending stress $\sigma(x)$ can be obtained as the following buckling formula:

$$\sigma(x) = -\frac{M(x)y}{I}. \tag{3}$$

The stress in a basic finite element is calculated as follows:

$$\begin{Bmatrix} \sigma_x \\ \sigma_y \\ \tau_{xy} \end{Bmatrix} = \begin{Bmatrix} \varepsilon_x \\ \varepsilon_y \\ \gamma_{xy} \end{Bmatrix} = E\boldsymbol{B}\boldsymbol{d}, \tag{4}$$

where $\boldsymbol{B}$ is the nodal strain displacement matrix and $\boldsymbol{d}$ is the nodal displacement vector. By calculating the stress of each known grid element, the global finite element strain equation can be solved and the stress can be calculated at any point within the element. In this study, the von Mises stress equation is used to analyze the stress of the designed electric motorcycle frame. For ductile materials, $\sigma_\varepsilon \le \sigma_\gamma$ is used to judge whether the stress is below the yield stress of the used material.

The von Mises stress equation can also be used to apply 1D results to 2D and 3D cases. The equation is

$$\sigma_e = \frac{1}{\sqrt{2}}\sqrt{(\sigma_1 - \sigma_2)^2 + (\sigma_2 - \sigma_3)^2 + (\sigma_3 - \sigma_1)^2}, \tag{5}$$

where σ_1, σ_2, and σ_3 are the three principal stresses at points considered in the structure. In the vector form of the 3D model, six independent stress components determine the stress state, and the independent components of strain in the vector form of stress are similar:

$$\sigma = \{\sigma\} = \begin{Bmatrix} \sigma_x \\ \sigma_y \\ \sigma_z \\ \tau_{xy} \\ \tau_{yz} \\ \tau_{zx} \end{Bmatrix}, \text{ or } [\sigma_{ij}] \text{ and } \varepsilon = \{\varepsilon\} = \begin{Bmatrix} \varepsilon_x \\ \varepsilon_y \\ \varepsilon_z \\ \gamma_{xy} \\ \gamma_{yz} \\ \gamma_{zx} \end{Bmatrix}, \text{ or } [\varepsilon_{ij}]. \tag{6}$$

The relational equation of the displacement surface is expressed as

$$u = \begin{Bmatrix} u(x,y,z) \\ v(x,y,z) \\ w(x,y,z) \end{Bmatrix} = \begin{Bmatrix} u_1 \\ u_2 \\ u_3 \end{Bmatrix}. \tag{7}$$

The stress and the volume force vector *f* at each point satisfy the following three equations to balance the elasticity problem:

$$\frac{\partial \sigma_x}{\partial_x} + \frac{\partial \tau_{xy}}{\partial_y} + \frac{\partial \tau_{xz}}{\partial_z} + f_x = 0, \frac{\partial \tau_{yx}}{\partial_x} + \frac{\partial \sigma_y}{\partial_y} + \frac{\partial \tau_{yz}}{\partial_z} + f_y = 0, \frac{\partial \tau_{zx}}{\partial_x} + \frac{\partial \tau_{zy}}{\partial_y} + \frac{\partial \sigma_z}{\partial_z} + f_z = 0. \tag{8}$$

The parameters of A36 structural steel used in the designed electric motorcycle frame are shown in Table 1, and the 3D model of the frame and the preliminary analysis points are shown in Fig. 1. The boundary conditions used in the preliminary analysis are shown in Table 2. The model shown in Fig. 1 is a good frame design and is thus used in further analyses.

Table 1
Parameters of A36 structural steel.

	Value	Unit
Density	7850	kg/m^{-3}
Young's coefficient	200	GPa
Poisson's ratio	0.3	
Bulk modulus	166.67	GPa
Shear modulus	76.92	GPa
Yield strength	250	MPa
Tensile strength	400	MPa

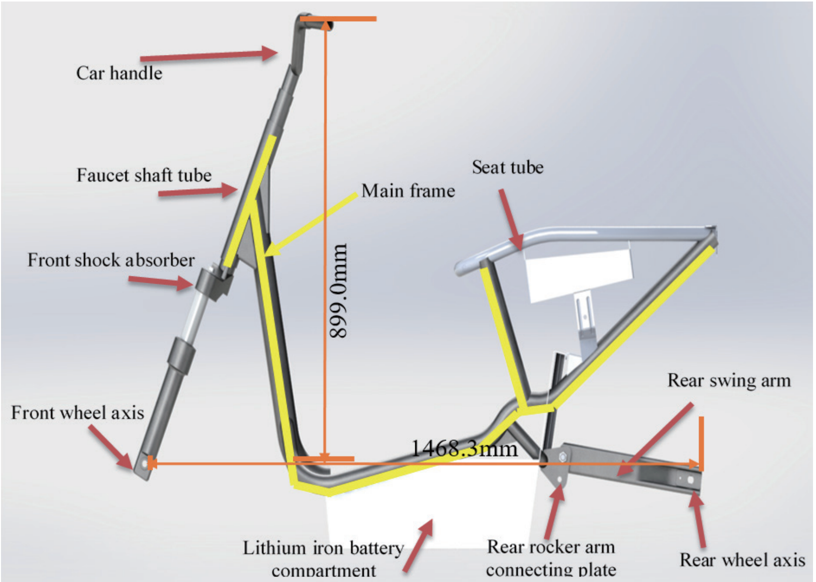

Fig. 1. (Color online) Structure of the 3D model for preliminary analysis.

Table 2
Boundary conditions in preliminary analysis.

Position	Boundary condition
Front wheel	Front axle constraint
Rear wheel	Rear axle constraint
Seat tube	Load 500 N

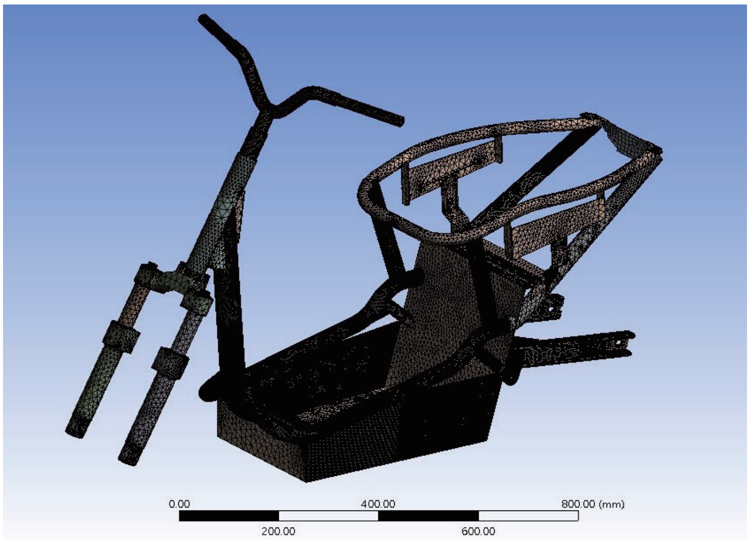

Fig. 2. (Color online) Grid of electric motorcycle frame.

The elements of the overall grid are shown in Fig. 2, and the grid numbers and elements for different positions are shown in Table 3. Figure 3 shows the densified area of mesh refinement at the connection between the head tube and main frame, and Fig. 4 shows the densified area of

Table 3
Description of grid.

	Complete frame	Number used for frame stiffness analysis
Nodes	2161306	525445
Grid elements	1112357	360695
Grid type	Tet10	

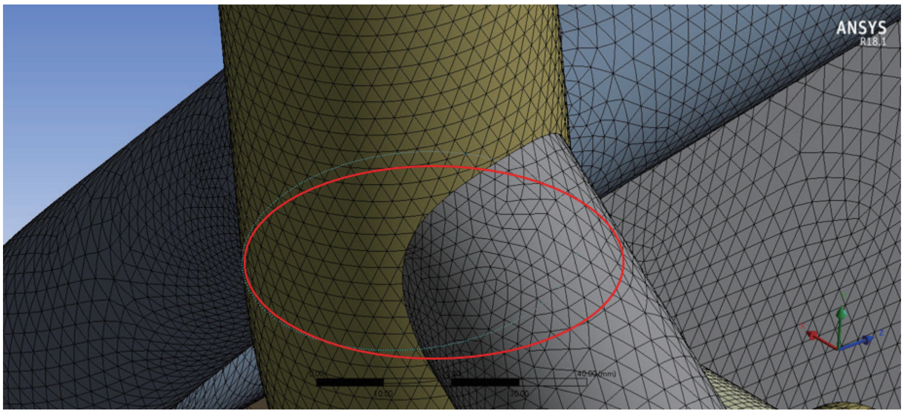

Fig. 3. (Color online) Densified area of mesh refinement at connection between head tube and main frame.

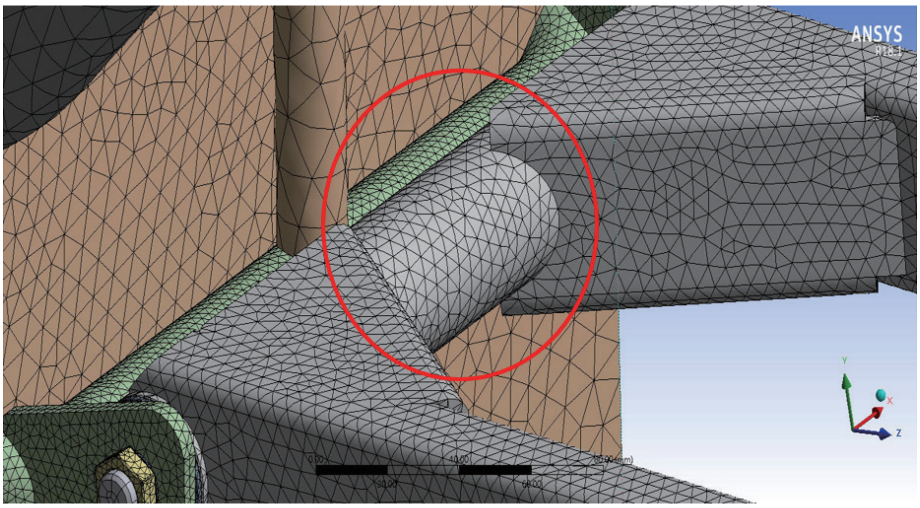

Fig. 4. (Color online) Densified area of mesh refinement at connection between main frame and seat tube.

mesh refinement at the connection between the main frame and seat tube. When the maximum stress, strain, or deformation occurs at the connection, the position can be displayed more accurately.

3. Simulation Results and Discussion

3.1 Grid convergence and divergence analyses

As shown in Fig. 5, the position of maximum stress found in the preliminary analysis was used as a reference point to test the analysis results of the convergence and divergence of the grids, as shown in Fig. 6. The results show that convergence occurred when there were about 920000 grid elements, for which the error of the calculation result was within 3%. Thus, 1.1 million elements were chosen for the grid in this study.

3.2 Axial force transmission analyses

The analysis of the axial force transmission path on the front of the electric motorcycle was based on FEM, and the results were used to discuss the force transmission mechanism in the

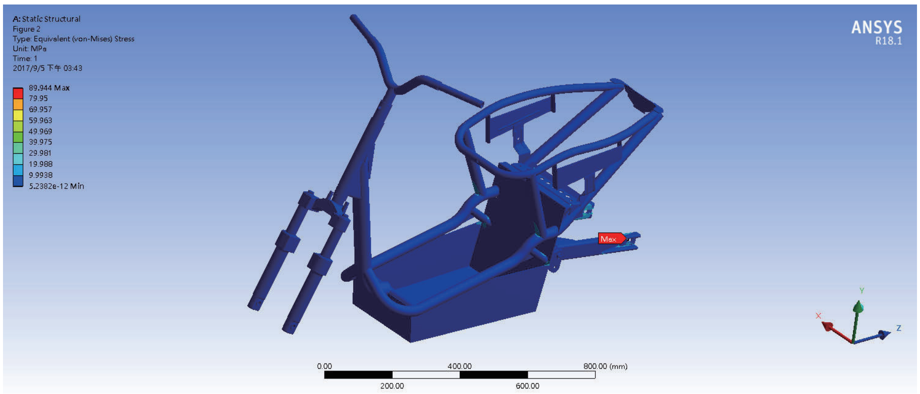

Fig. 5. (Color online) Reference point of the maximum stress position.

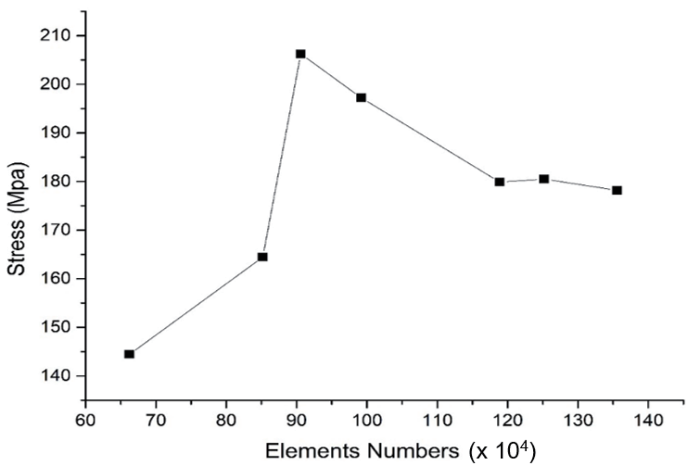

Fig. 6. Mesh convergence curve.

frame structure. We analyzed and set the stress transmission path with the main aim of finding the designed load conditions and three different constrained boundary conditions. The boundary conditions when the front and rear wheel axles were constrained are shown in Fig. 7. The transmission path and bending moment were combined with the constraint of the front wheel axle, and the maximum stress was transferred to the position of the handlebar.

3.3 Axial force of front wheel when front wheel axle was constrained

For the boundary condition that the front wheel axle was constrained, the stress and bending moment were transmitted to the rear end of the frame through the axle tube and then to the battery compartment at the bottom of the frame. The transmission path was from the faucet shaft tube to the rear wheel shaft and the seat tube, as shown in Fig. 8.

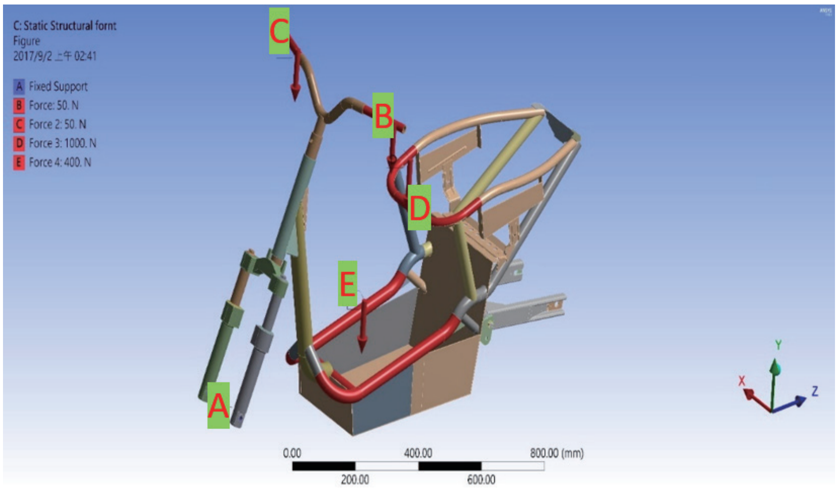

Fig. 7. (Color online) Boundary condition when front and rear wheel axles were constrained.

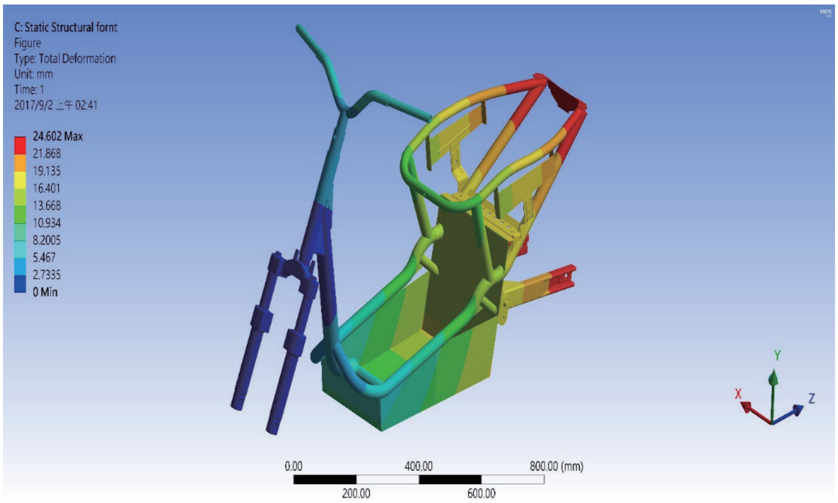

Fig. 8. (Color online) Force transmission path when the front wheel axle was constrained.

3.4 Front axle force when rear wheel axle was constrained

For the boundary condition that the rear wheel axle was constrained, as shown in Fig. 9, the stress and bending moment first passed through the rear rocker arm and the bottom battery compartment to the reinforced ribs. The transmission path from the battery compartment and the frame to the front wheel axis and the handlebar is shown in Fig. 10.

3.5 Axial forces when both front and rear wheel axle centers were constrained

The boundary conditions for the constraint of the front and rear wheel axle centers are shown in Fig. 11 and the transmission path is shown in Fig. 12. Since the axle centers of the front and rear wheels were constrained, the force was mainly transmitted to the handlebar and seat tube.

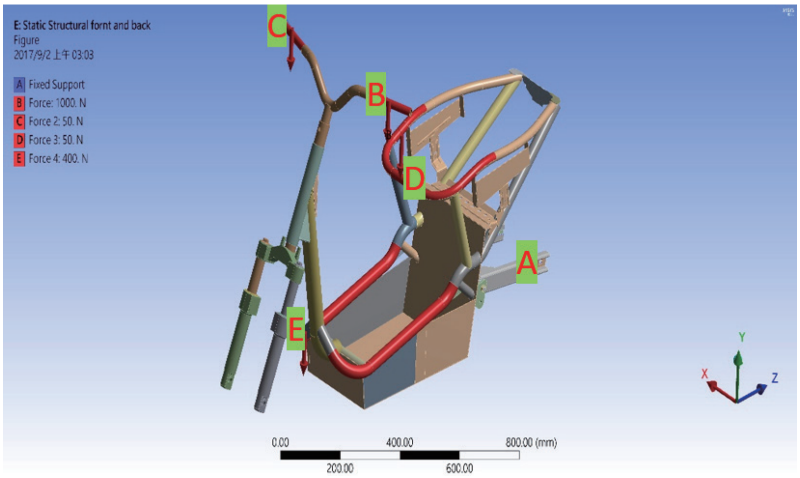

Fig. 9. (Color online) Boundary condition when rear wheel axle was constrained.

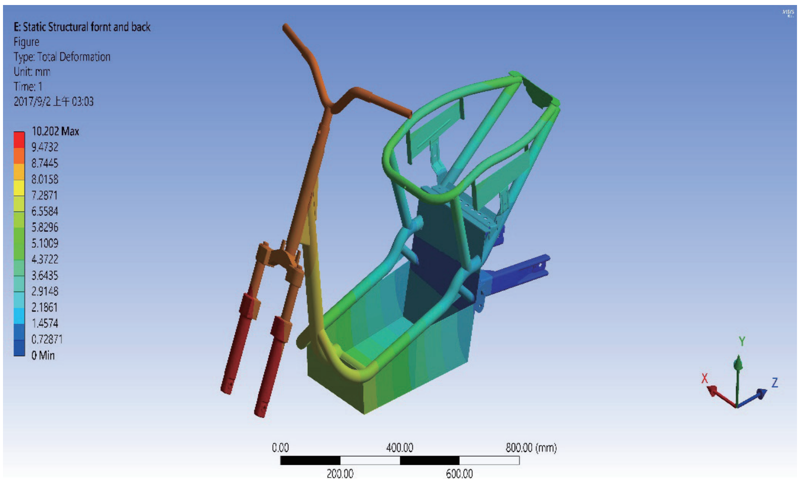

Fig. 10. (Color online) Axial force transmission path when rear wheel axle was constrained.

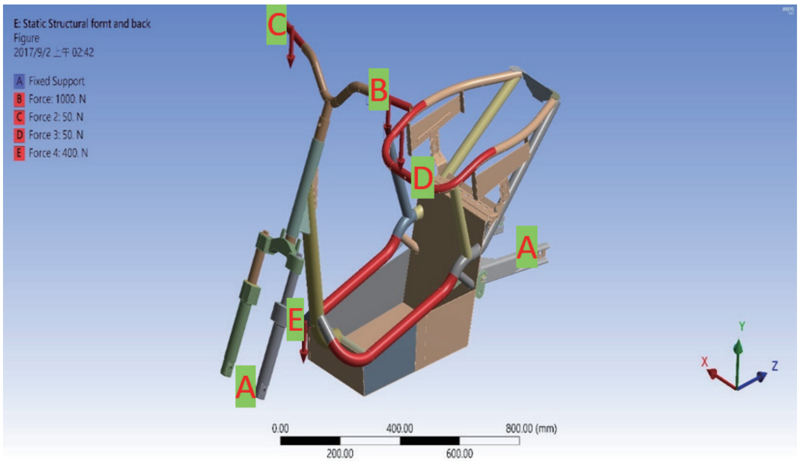

Fig. 11. (Color online) Boundary conditions when both front and rear wheel axle centers were constrained.

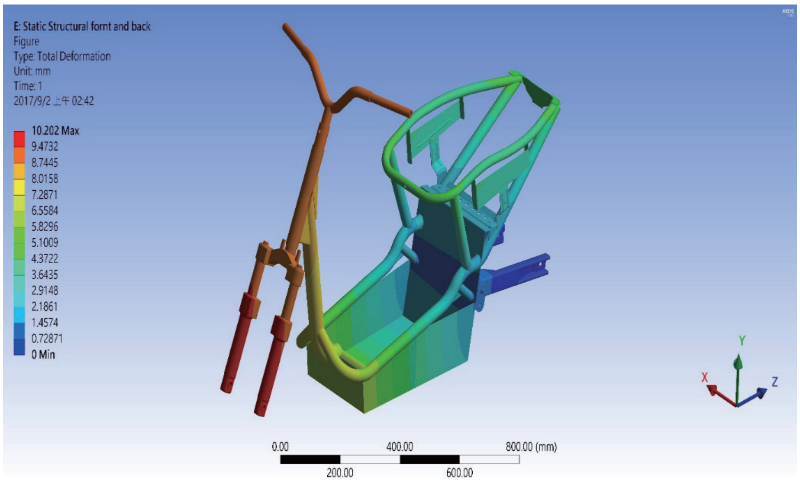

Fig. 12. (Color online) Axial force transmission paths of axle centers when front and rear wheel axles were constrained.

3.6 Analyses of up and down bending moment stiffnesses, left and right bending moment stiffnesses, and front and rear bending moment stiffnesses

When an electric motorcycle is being driven on a road, it encounters different road conditions, such as rough areas and potholes, and when it turns, the frame is subjected to bending and torsion loads. The aforementioned load conditions encountered during driving are transmitted from the front shock absorber to the head tube, then from the head tube to the frame structure. Therefore, it is necessary to simulate the force transmission mechanism to confirm that the design can distribute the loads rather than concentrate the stresses. If the frame is insufficiently rigid, its deformation will be too large, which will cause difficulties during riding and even affect the stability of the motorcycle. Therefore, the rigidity and strength of the frame structure are important factors in the design of electric motorcycles.

As reported in this section, the torque and bending moment stiffness of the frame were analyzed. In the setting of the boundary conditions, the model of the frame was fixed to the position of the front wheel axle, meaning that the degrees of freedom in the *x*-, *y*-, and *z*-axis directions and the degrees of freedom in the *x*-, *y*-, and *z*-axis rotations were fixed. The model of the rear rocker arm was also set in contact with the rigid body and fixed to the rocker arm of the rear wheel, which fixed its degree of freedom. Because the frame design in this study used twin shock absorbers, the rear rocker arm adopted a bilateral suspension mode. The configuration of the bilateral suspension reduced the unbalanced force, which was generated at the rear rocker arm and caused by the structure of the unilateral suspension.

Because our aim was to explore the force acting on the frame, the welding or bolt connections were neglected. The frame was treated as having a perfect connection, and the grid encryption setting was used to ensure that the calculation of the connection was accurate. In the analysis, we used a simplified model with the frame strength of the most fundamental design. The bending stiffness of the frame was defined as the bending angle when the frame was subjected to a force parallel to the frame head tube. The stiffness of the bending object was calculated as the product of the applied bending moment load and the radius of curvature of the bending angle, and the unit was N-m. Torque rigidity was defined as the torsion angle generated when the frame head tube was subjected to a force perpendicular to the axis of the faucet shaft tube. Since the frame was designed to be symmetrical, it was only necessary to analyze the bending moment in one direction. Torque stiffness was calculated by dividing the applied torque by the torsion rate in N-m/rad. The boundary conditions used in the analysis of the bending moment stiffness are shown in Fig. 13. The positions of the maximum up and down bending moment deformations, the positions of the maximum left and right bending moment deformations, and the positions of the maximum front and rear torque stresses are shown in Figs. 14–16. The stresses for the maximum deformation positions generated by the up and down bending moments, the maximum deformation positions caused by the left and right bending moments, and the positions of maximum stress caused by the front and rear torques were obtained from these simulation images.

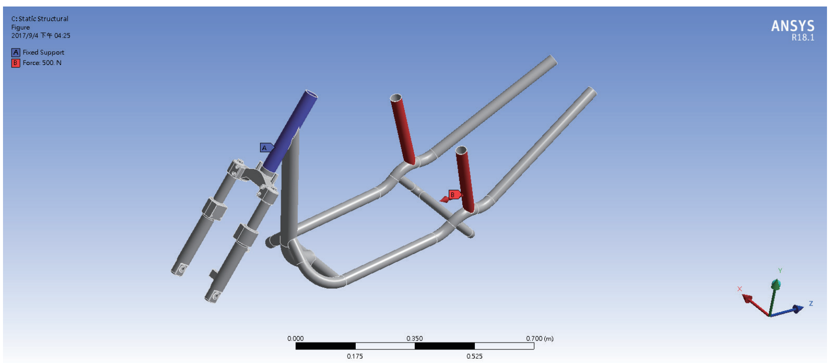

Fig. 13. (Color online) Boundary conditions of upper and lower bending moment stiffnesses.

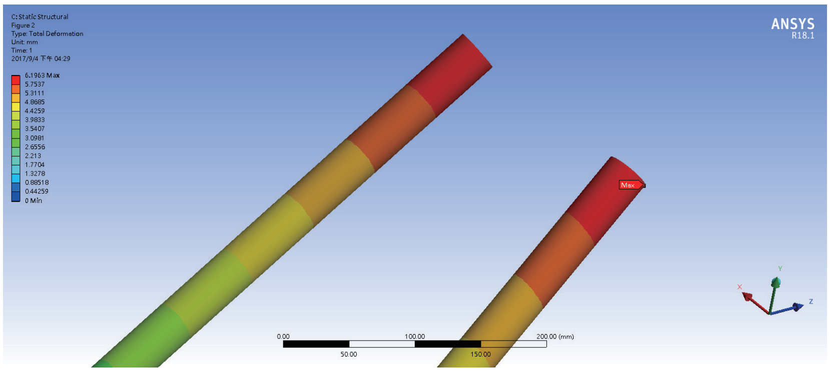

Fig. 14. (Color online) Positions of the maximum up and down bending moment deformations.

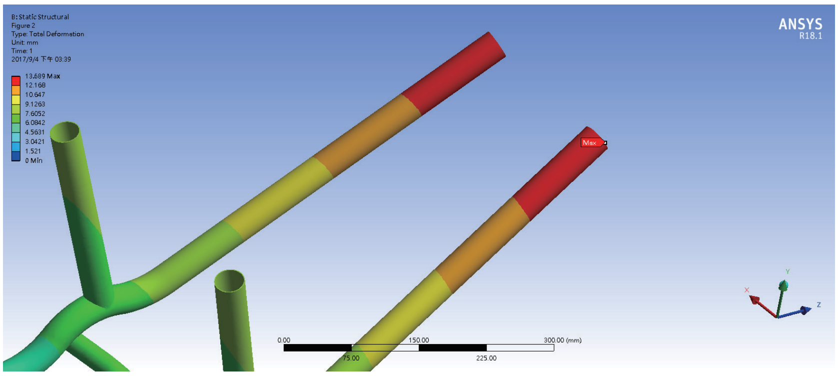

Fig. 15. (Color online) Positions of the maximum left and right bending moment deformations.

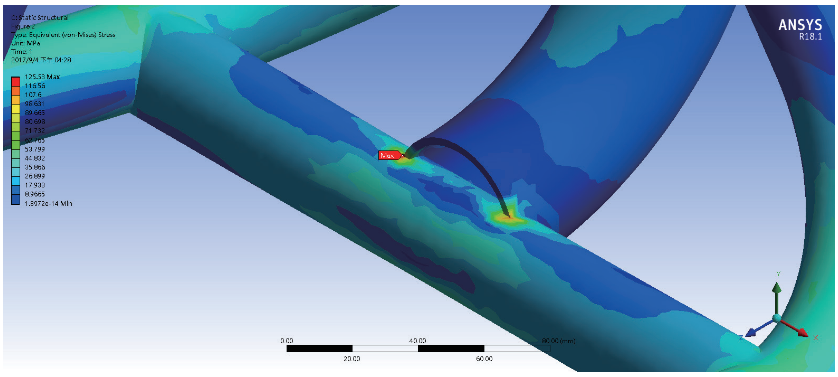

Fig. 16. (Color online) Positions of the maximum front and rear torque stresses.

4. Conclusions

In this study, A36 structural steel was used to design an electric motorcycle frame, and ANSYS was successfully used as FEM software to simulate and analyze a newly designed electric motorcycle. Convergence occurred when there were about 920000 grid elements, for which the error of the calculation result was within 3%. Thus, 1.1 million elements were chosen for the grid in this study. After the validity of the structure of the newly designed electric motorcycle was confirmed, we performed various analyses, including of the axial force transmission, the force transmission path when the front wheel axle was constrained, the axial force transmission path when the rear wheel axle was constrained, and the axial force transmission paths of the axle centers at when the front and rear wheel axles were constrained. We also analyzed the up and down bending moment stiffnesses, left and right bending moment stiffnesses, and front and rear bending moment stiffnesses.

Acknowledgments

This work was supported by projects Nos. MOST 110-2622-E-390-002 and MOST 110-2221-E-390-020.

References

1 Ministry of communications statistical inquiry network - Ministry of communications of Taiwan: https://stat.motc.gov.tw/mocdb/stmain.jsp?sys=100&funid=a3301 (accessed 12, 2021).
2 S. Matey, D. R Prajapati, K. Shinde, A. Mhaske, and A. Prabhu: Int. J. Mech. Eng. Technol. **8** (2017) 245.
3 M. Vignesh, K. Arumugam, S. Vinoth, and S. Hariharan: Int. J. Eng. Sci. Invent. **8** (2019) 2319.
4 R. Tuluie and G. Ericksen: SAE Technical. Paper 2000-01-3576 (2000).
5 A. O. Kiyakli and H. Solmaz: Int. J. Automotive Sci. Technol. **2** (2018) 9.
6 P. Wang, X. Tan, G. Wang, J. Li, Q. Su, C. Shen, and Y. Zhang: Soft Comput. **25** (2021) 12453.
7 K. B. Sheu: Appl. Energy **84** (2007) 1289.
8 M. A. B. Marzuki, M. A. A. Bakar, and M. F. M. Azmi: Int. J. Inf. Syst. Eng. **1** (2015) 2265.